

Mathematical formulation using experimental study of hydrodynamic forces acting on substructures of coastal pile foundation bridges during earthquakes: As a model of human bridge protective

By

Riyadh Alsultani*

Department of Civil Engineering, University of Technology, 10011, Baghdad, Iraq,

*Corresponding author: *E-mail address:* bce.19.52@grad.uotechnology.edu.iq

Ibtisam R. Karim

Department of Civil Engineering, University of Technology, 10011, Baghdad, Iraq,

Email: 40049@uotechnology.edu.iq

Saleh I. Khassaf

Department of Civil Engineering, University of Basrah, 61001, Basrah, Iraq,

Email: Saleh.Khassaf@uobasrah.edu.iq

Abstract

The substructures of sea-crossing pile foundation bridges, which are located in zones with active seismicity, are vulnerable to earthquakes and water forces that induce damage during their beneficial operation. This study investigated the behavior of this type of bridge under the combined influence of water forces represented by currents and waves during seismic actions. This study proposed a method for analyzing Morison equation and simplified its inertial and drag coefficients. A new technique called the reality water-structure-earthquake interaction test (RWSEIT) has been developed to study the hydrodynamic pressure distribution and acceleration along the height of the pile foundation of a 1:20 scale concrete model. To find Morison coefficient values, the changing rule of hydrodynamic pressure with water depths, current speed, wave properties, earthquake amplitudes, and earthquake frequencies is studied. The results proved that the inertial coefficient has the same changing rule as the drag coefficient. The inertial coefficient ranged from 0.117 to 1.950 and the drag coefficient ranged from 0.017 to 0.230 under various studied conditions. Finally, a statistical analysis was carried out based on the results from the tests, and two equations for the inertial and drag coefficients were introduced, with correlation coefficients of 0.9 and 0.92, respectively.

Keywords: Hydrodynamic pressure distribution; Morison equation; Drag and inertial coefficients; Bridge pier; Pile foundation; Current-wave-earthquake.

1. Introduction

Globally, the construction of coastal structures such as sea-crossing bridges has increased in recent years. Among them are those bridges located in deep water and earthquake zones, which need an intensive study on the effect of the fluid-structure-earthquake interaction. Moreover, the earthquake may apply the wave and current load simultaneously to the submerged parts of bridges in deep water. It is well known that fluid-structure interaction (FSI) produces an additional hydrodynamic force on the structure when it vibrates in water. The additional hydrodynamic force could modify the dynamic properties of the structure and result in structural damage. The wave-current loading has the potential to cause further damage to bridges.

Morison equation has been widely used to calculate the hydrodynamic pressure on coastal structures. Many researchers have investigated the inertial and drag coefficients in the Morison equation for wave force. However, there is hardly any study on the coefficients in the Morison equation for earthquake-induced hydrodynamic pressure in terms of wave and current forces.

To compute the wave force of a small diameter cylinder, Morison et al. (1950) proposed a semi-empirical formula. The assumption is that the cylinder does not influence the wave's movement. Penzien and Kaul (1972) developed the Morison equation to calculate the hydrodynamic pressure of small diameter cylinders during earthquakes and used the stochastic method and response spectrum method to analyze the dynamic response of four representative deep-water towers during strong earthquakes. Using the Morison equation, Li et al. (2010) investigated the effect of hydrodynamic pressure on the response of the large group piles foundation of the Yangtze River Road bridge. Martinelli et al. (2011) investigated the dynamic performance of submerged floating tunnels during earthquakes, taking into account the excitation's spatial variability and the fluid-structure interaction, and using the Morison equation to compute the hydrodynamic pressure. Yang and Li (2013) used an expanded Morison equation to determine the hydrodynamic pressure caused by inner water in hollow columns during earthquakes. Inner water's hydrodynamic force was represented as an inertial force induced by the increased mass of the inner water. The expressions of hydrodynamic pressure for cylindrical hollow piers induced by outside water and inner water were changed and simplified by Li and Yang (2013). The results demonstrated that the hydrodynamic pressure impact affected the seismic response characteristics and that the FSI should be addressed for coastal structures subjected to earthquakes, with the Morison equation being the primary approach for calculating the hydrodynamic pressure owing to FSI.

Vengatesan et al. (2000) studied the hydrodynamic coefficients of a vertical truncated rectangular cylinder owing to regular and random waves in tests. In regular waves, Yuan and Huang (2010) explored the in-line force on a small slice of a vertical circular cylinder of various truncated lengths, and the inertia and drag coefficients were reported as a function of the Keulegan-Carpenter number. Simulated drag and inertia coefficients for a circular cylinder in steady and low-amplitude oscillatory flows were explored by Konstantinidis and Bouris (2017), and the coefficients in the Morison equation were calculated using the least-squares approach. In irregular waves, Raed and Soares (2018) investigated the influence of drag and inertia coefficients on the Morison wave force operating on a stationary vertical cylinder. Zhong et al. (2019) investigated the inertial coefficient in the Morison equation for earthquake-induced hydrodynamic added mass by performing a series of dynamic experiments on four steel tubes of various diameters. The Reynolds number, Keulegan-Carpenter number, water depth, aspect ratios (Diameter/Length) of the cylinder, and the relative roughness of the structure surface were the five key parameters that influenced the inertial and drag coefficients, according to the findings.

Wei et al. (2013) showed that FSI had a substantial impact on the dynamic response of bridge pile foundations submerged in water in their experiment. Zheng et al. (2015) conducted an experimental investigation on a mono-pile wind turbine foundation to evaluate the combined action of powerful earthquakes and moderate sea conditions. Liu et al. (2017) investigated the combined earthquake, wave, and current action on a pile group cable-stayed bridge tower foundation in an experimental investigation. Ding et al. (2018) evaluated the influence of wave-current action on the seismic responses of a pier and the distribution law of hydrodynamic pressure along the height of the pier under various water load circumstances using underwater shaking table experiments. Under hurricane-generated water waves, Fang et al. (2018) developed an analytical solution for hydrodynamic wave forces acting on girder-type bridge decks. Wang et al. (2019) studied the dynamic response of a circular pier with a rigid base under combined earthquake and wave-current activities.

Under wave-current-earthquake conditions, An-jie and Wan (2020) developed a computational model to evaluate the hydrodynamic force on a pile within a pile-group foundation of a sea-crossing bridge. The following is a summary of the findings from the previous studies: The influence of fluid-structure interaction on submerged portions rises with water depth; the hydrodynamic pressure was first, second, and third, respectively, due to the earthquake, wave, and current. The highest hydrodynamic pressures are found at the water's surface, and they progressively diminish from the surface to the bottom of the water. The wave force may have a greater effect on the displacement of the pier when the earthquake action is relatively small, which is more significant when the wave height is larger and the peak ground acceleration is smaller; the wave force may have a greater effect on the displacement of the pier when the earthquake action is relatively small, which is more significant when the wave height is larger and the peak ground acceleration is smaller. The wave force, on the other hand, has minimal influence on the pier's acceleration; when the pier is subjected to combined earthquake and wave-current action, the coupling effect determines whether the wave-current action raises or reduces the pier's peak seismic reactions.

This paper conducted a series of hydrodynamic tests on pile foundation bridge pier subjected to combined current, wave, and earthquake actions in a newly designed test called reality water-structure-earthquake interaction test (RWSEIT). First, the hydrodynamic water pressure for a 1/20 scaled concrete model with nine piles, elevated pile cap, single rectangular pier, and hammerhead superstructure, was examined. Second, proposed an analytical method for the Morison equation for the hydrodynamic pressure distribution along the height of the upstream central bridge pile; Third, the changing rule of hydrodynamic pressure with water depths, current velocities, wave properties, earthquake amplitudes, and earthquake frequencies, is studied; Fourth, the inertial and drag values in the Morison equation then determined. Finally, two equations for the inertial and drag coefficients were introduced, using correlation statistical analysis.

2. Test System and Model Design

The experiments were carried out using a system developed by the Civil Engineering Laboratory at the University of Technology – Iraq called Reality Water-Structure-Earthquake Interaction Test (RWSEIT). The system is designed to simulate current, wave, and earthquake activities independently or dependent on the same system. The test equipment consists of a wave-current flume with dimensions of 6.0 x 1.50 x 1.25 m and a horizontal bi-axial shaking actuator below it, as illustrated in Figure 1(a).

At the upstream end of the flume, a flap-type wave maker (Figure 1b) is installed across the width of the tank. A stepper-controlled electric motor drives the flap. In the frequency range of 0.4–1.4 Hz, the wave generator can create both regular and random waves. The maximum wave height is 0.2 m, and the test wave period is 0.5 to 4 seconds.

An electro-mechanically controlled Positive Displacement Pump with three discharge pipes and three suction pipes with diameters of about 19.5 cm is also included in the system. The flume's peak current speed may reach 0.5 m/s.

The shaking device, which is positioned in the center of the flume and has a square form with dimensions of 1.5x1.5 m, may shake in x and y horizontal directions as well as pitch directions. The shaking table has dimensions of 1.0x1.0 m and is linked to the center of the bottom of the water tank using waterproof fabric, as shown in Figure 1(c). 2 tonnes, 100 mm, 2.0 g, and 40 Hz are the maximum table load capacity, displacement, acceleration, and frequency, respectively.

An angled mesh plate (Figure 1d) is installed at the flume's downstream end to absorb the energy

of arriving currents-waves, and the plate efficiently dissipated the majority of the incoming energy.

A pile foundation has been applied widely for deepwater sites to ensure stability against earthquakes, waves, and currents during their service period, so the sea-crossing coastal bridge of Songhua River in northeast China (Wei et al., 2013) is taken as the prototype structure. This bridge is composed of nine piles, elevated pile caps, a single rectangular pier, and a hammerhead superstructure and as shown in Figure 2. The total length of the piles is 58 m, with a segment 12 m above the scour line.

The gravitational and inertial forces should be fulfilled jointly in this study since it focuses on the dependent action of current, wave, and earthquake on a pile foundation bridge. As a result, to replicate the hydrodynamic features and similitude connections between prototype and model, Froude and Cauchy numbers must be used in testing (Harris and Sabnis 1990; Gao et al., 2000). The geometric scale factor was chosen as 20 due to the proportions of the wave-current tank and shaking table. The reduced scale model is made of reinforced concrete and the bridge deck's influence on the superstructure is simplified as a concentrating mass on the top of the pier utilizing heavier steel material in the smaller scale model, which is composed of reinforced concrete.

The geometry of the model is shown in Figure 3, and a steel plate with $0.6 \times 0.6 \times 0.02$ m was used on the bottom of the model to connect the shaking table. Mass blocks were added to the top of the model, and the total mass was 54.225 kg.

The natural frequencies of the model are compared to those of the prototype in this investigation to verify the similitude relationships and model design (Table 1). ABAQUS finite element software was used to do the modal analysis. The findings showed that the differences between the prototype and the model are minor, with a maximum value of less than 4%, indicating that the model design is reliable

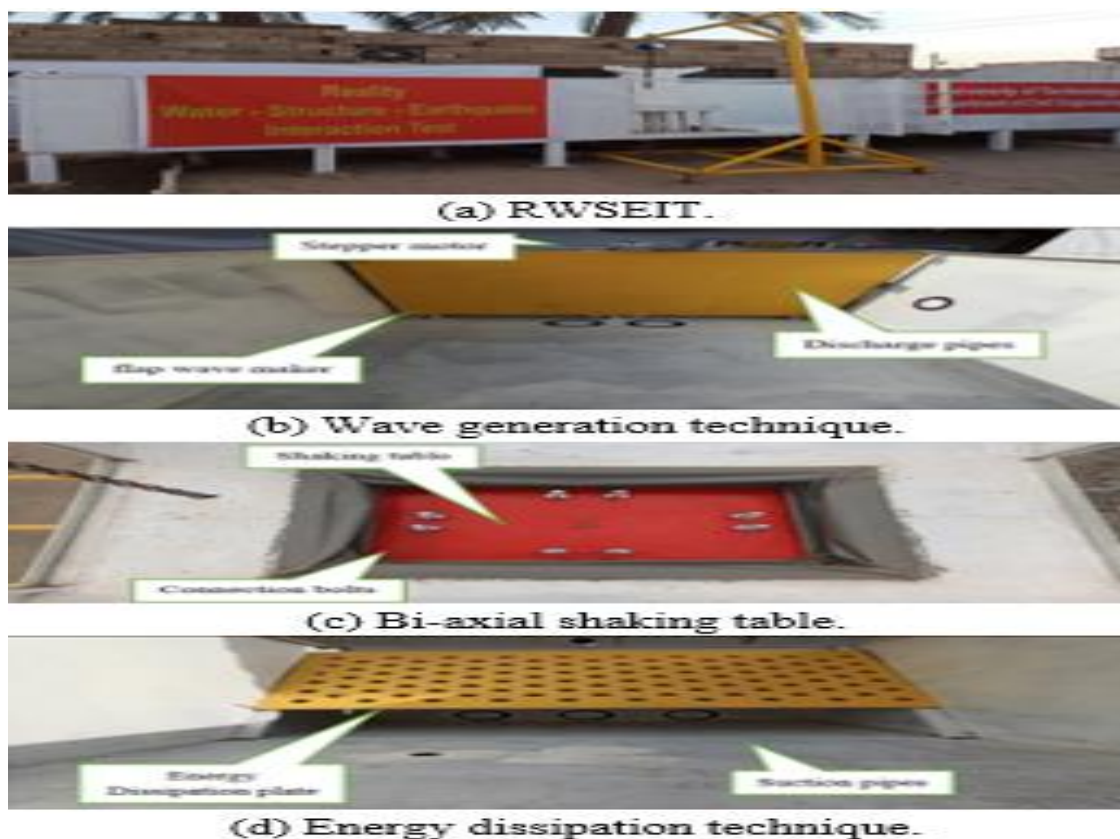


Figure 1 Components of the designed system (RWSEIT).

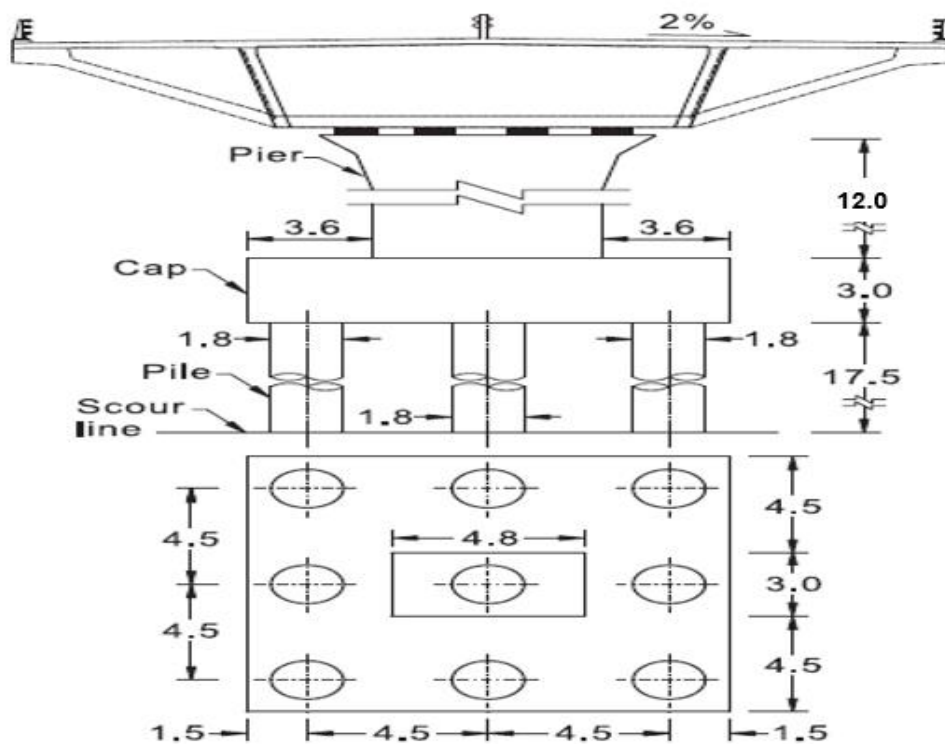


Figure 2 Sea-crossing bridge of Songhua River in northeast China (Wei et al., 2013).



Figure 3 Model geometry.

Table 1. Verification of the frequency similitude relation between prototype and model.

Mode	Prototype (Hz)		Model (Hz)	Error (%)
	f_p	f_p/S_f	f_m	
1	0.8	3.57	3.48	2.58
2	2.48	11.09	10.88	1.93
3	3.68	16.45	15.84	3.85
4	6.24	27.91	27.45	1.67

3. Test Conditions

Morison equation shows that the earthquake-induced hydrodynamic pressure depends on water forces, earthquake accelerations, and structure geometries. Many studies indicate that the inertial and drag coefficients of Morison are related to water depth, current speed, and wave properties. Therefore, to comprehensively analyze these coefficients, a series of tests on pile foundation bridges with different water depths, current speed, depth-length-period of the wave, and input action frequencies-amplitudes of the earthquake, are conducted.

There are three water levels are considered in the tests, i.e. 0.3, 0.45, and 0.6. Moreover, three different specifications of uniform current speed with three different characteristics of the regular wave were selected as shown in Table 2.

To study the changing rule of the hydrodynamic pressure, inertial and drag coefficients according to the input action frequency and amplitude, the real acceleration time histories of the Halabjah, Iraq earthquake (2019) in Baghdad (Al-Taie and Albusoda 2019), were chosen as the input earthquake excitation. The original accelerogram has a total ground excitation time history of 205 seconds with a peak ground acceleration (PGA) of 1.0g at 41.5 seconds, as shown in Figure 4 (a). To prevent the model from being damaged due to the cyclic earthquake loading, three frequencies 5, 10 and 20 Hz, and three amplitudes 0.05g, 0.1g and 0.2g, were selected as input loadings in the test. The duration time was adjusted according to the time scale factor, which is about 45.85 seconds. Figs. 4 (b, c and d) gives the characteristics of the selected earthquake excitations 0.05g, 0.1g and 0.2g, respectively.

Table 2. Applied conditions in the test.

Water depth (m)	Current speed (m/sec)	Wave properties (depth m, length m period sec)	Earthquake Amplitudes (g)	Earthquake Frequencies (Hz)
H1 0.30	C1 0.1	W1 0.02, 0.1, 2	A1 0.05	F1 2
H2 0.45	C2 0.2	W2 0.02, 0.2, 1	A2 0.10	F2 4
H3 0.60	C3 0.4	W3 0.03, 0.1, 1	A3 0.20	F3 8

In conclusion, to obtain certified hydrodynamic coefficients for the Morison equation, there are 234 simulated test cases performed in total.

4. Test Data Acquisition

The test recorded acceleration and hydrodynamic pressure along the submerged height of the pile, as well as current and wave parameters in the flume. The acceleration transducers feature a waterproof frame and may be used to monitor acceleration underwater. The waterproof point pressure gauge measures the hydrodynamic pressure. The location of measurement devices along the specimen is shown in Figure 5. There are (5) point pressure transducers and (5) acceleration transducers. Because

the acceleration and hydrodynamic pressure at the downstream face is the same as at the same height of the downstream face, the acceleration and point pressure transducers are put at the downstream and upstream faces of the specimen, respectively.

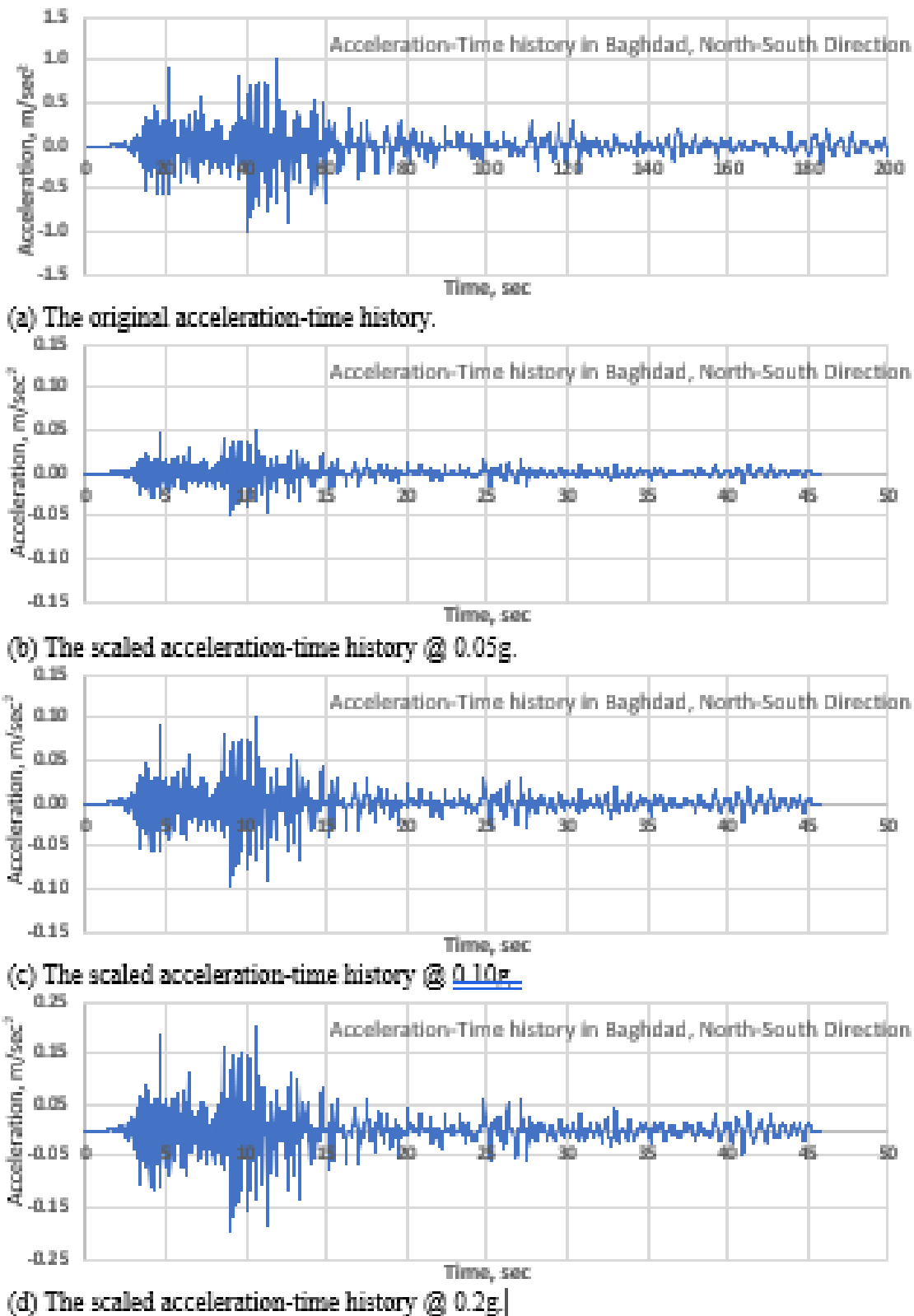


Figure 4 Acceleration time history of Halabjah earthquakes in Baghdad.

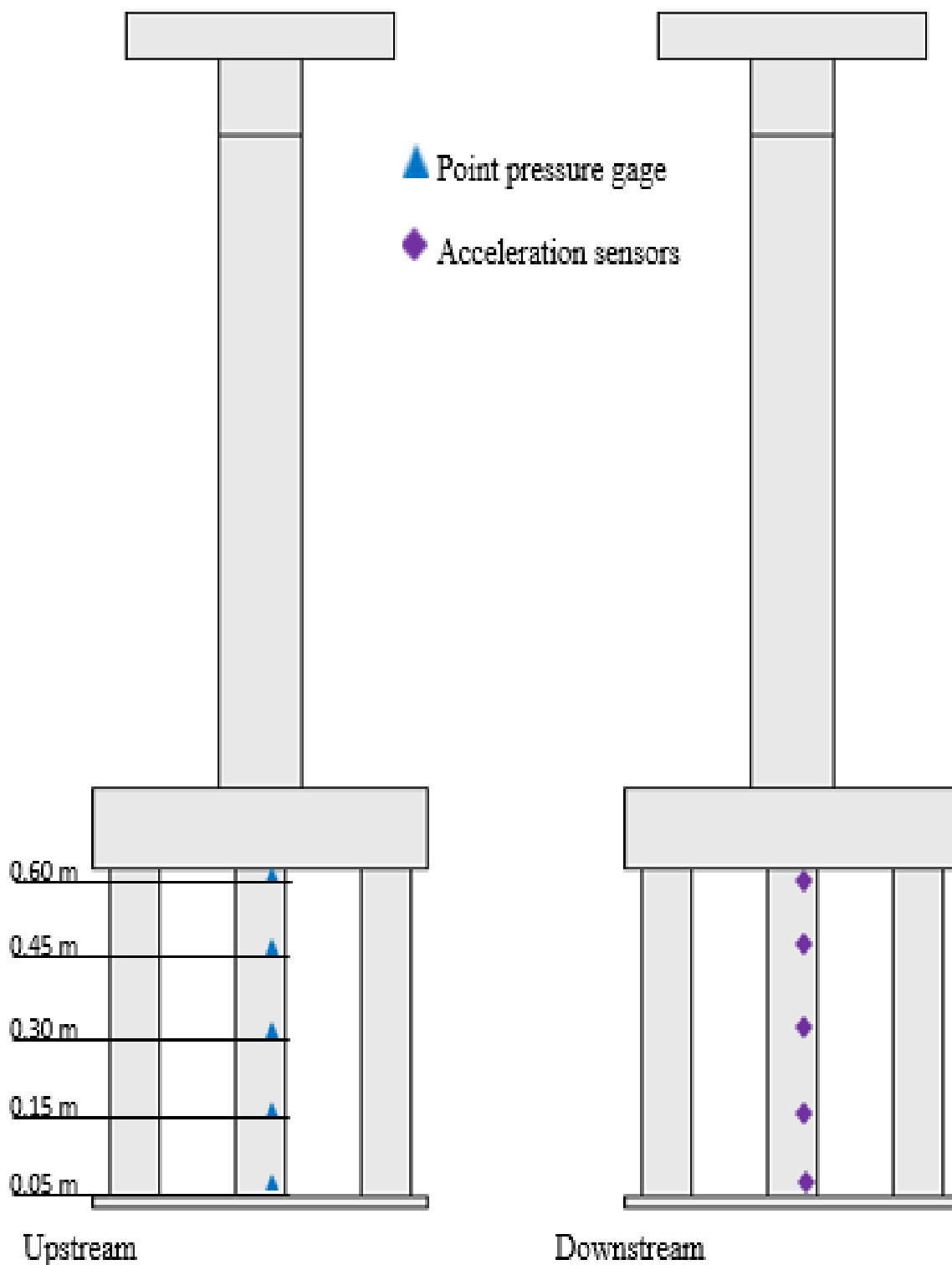


Figure 5 The layout of measuring sensors.

5. Test Results and Analysis

To investigate the solution of the hydrodynamic force owing to combined current, wave, and earthquake action, the Morison equation was developed. The total hydrodynamic force's changing rules were explored with water depths, current speed, wave properties,

earthquake frequencies, and amplitudes.

According to (Zhong et al., 2018) Morison equation of hydrodynamic force per unit height, P , can be presented as shown in Eq. (1)

$$P = \frac{1}{2}C_D\rho_f D|\dot{u} - \dot{x}_0|(\dot{u} - \dot{x}_0) + \frac{\pi}{4}\rho_f C_M D^2(\ddot{u} - \ddot{x}_0) + \rho_f A\ddot{u} \quad (1)$$

where ρ_f is the density of water; C_D and C_A are the drag and inertia force coefficients, respectively; D and A are the diameter and area of the exposed face, respectively; \dot{x}_0 and \ddot{x}_0 are the absolute velocity and associated acceleration of the structure, respectively; and \dot{u} and \ddot{u} are the velocity and associated acceleration of water, respectively.

The first term at the right of Eq. (1) denotes the drag force, the second term denotes the inertial force, and the third term denotes the structural effect.

For coastal and offshore structures, the influence of hydrodynamic drag force, represented by combined wave and current actions, on the dynamic response of structures is very important (Goto and Toki, 1965; Song et al., 2013). Therefore, the Morison equation can be modified to account for waves and currents by replacing ' \dot{u} ' by ' $C + W$ ', where C is the water current speed and W is wave properties as presented in Eq. (2)

$$P = \frac{1}{2}C_D \rho_f D|(C + W) - \dot{x}_0|((C + W) - \dot{x}_0) + \frac{\pi}{4}\rho_f C_M D^2(\ddot{u} - \ddot{x}_0) + \rho_f A\ddot{u} \quad (2)$$

The drag coefficient is calculated by simplifying the drag force presented in the first part of the Morison equation (Eq.1) as the following expressions (Eq.3):

$$C_D = \frac{M}{\frac{1}{2}\rho_f D h |(C+W) - \dot{x}_0| ((C+W) - \dot{x}_0)} \quad (3)$$

where h is the water depth. As shown in Eq. (3), the hydrodynamic drag coefficient is proportional to h and D and independent of the current and wave of water.

A lift force is also connected with the loading on a bridge's submerged components, in addition to the drag force. Because of the orbital motion of the water particles, this lift force is perpendicular to the velocity vector and rotates around the axis of the members. However, because the magnitude, direction, and duration of the lift force are unknown, they cannot be included in Morison's equation, and the influence of vortex shedding will appear as noise in drag and inertia component measurements (Teng and Nath 1985).

The second part of Eq. (2) is justified to calculate the inertia coefficient and as shown below (Eq. 4):

$$C_M = \frac{M}{\frac{\pi}{4}\rho_f D^2 h (\ddot{u} - \ddot{x}_0)} \quad (4)$$

As shown in Eq. (4), the hydrodynamic mass is proportional to h and D^2 and independent of the action of frequency and amplitude.

This study aimed at the hydrodynamic forces exerted on submerged bridge parts in non-quiet water during earthquakes, while the effect of structures on the movement of water is

neglected; therefore the third part will be removed from the modified Morison equation.

The absolute velocity and related acceleration of the water and structure may be estimated utilizing high-speed data transmission acquisition, which is something that must be clarified (DAC). This DAC has been employed as a sensor output data reader and can do internal first and second data integration (Waveform Characteristics). To do this, the motion sensor (accelerometer) may be used to read the output acceleration and then perform first and second integration to obtain the associated velocity and displacement at the given places.

5.1. Results with different current speed

The experimental model was subjected to a series of consciously selected tests to find out what is the most influential factor.

The selected three water depths (H1, H2 and H3) m were set as constant parameters in the study of the effect of the conditions studied in this subsection and the following subsections (5.2 to 5.4). As for the other variables, they were chosen as appropriate for the cases that can be found mostly in the practical sites. Water wave W3, current speed C3, earthquake amplitude A3, and earthquake frequency F3, were taken as constant studied variables, to focus analysis on the hydrodynamic response of the bridge foundation.

The effect of different actions of water currents (0.1, 0.2 and 0.4) m/sec under the three water depths (0.3, 0.45 and 0.6) m, are studied with constant properties of wave, earthquake amplitude and earthquake frequency. Therefore, the inertial and drag coefficient of C1W3A3F3, C2W3A3F3 and C3W3A3F3, were presented in Figs. 6 (a, b and c).

The three Figures show that the effect of the water current increases the inertial and drag coefficients in a distinctive and equal manner for all the currents studied in this research. Also, the increase of the current speed is almost greater by 31%, 68% and 100% with the increase in the values C1, C2 and C3, respectively.

The hydrodynamic pressure of the pile increases from bottom to top and for all the studied water heights, this is due to the effect of the height of the water column. That is the compressed mass of water as a result of currents increases from the bottom to the surface.

In general, it can be seen that the inertial coefficient has the same changing rule as the drag coefficient. Take the inertial coefficient as an example, it can be noted that the coefficient changed relatively small with the increase in current speed. For all the curves in Figs. 6 (a, b and c), the change of hydrodynamic pressure was less than 10% as the current increasing from 0.1m/sec to 0.4m/sec.

Note that the results of other conditions, of waves-amplitudes-frequencies, had similar behavior to the results listed here.

The effect of current for other conditions of waves, amplitudes and frequencies, were appeared with similar behavior to the results listed here. The results indicated that the increase of the current speed is almost greater by 4%, 12% and 15% with the increase in the values of

the wave, amplitude and frequency, respectively as the current speed increases from C1 to C3.

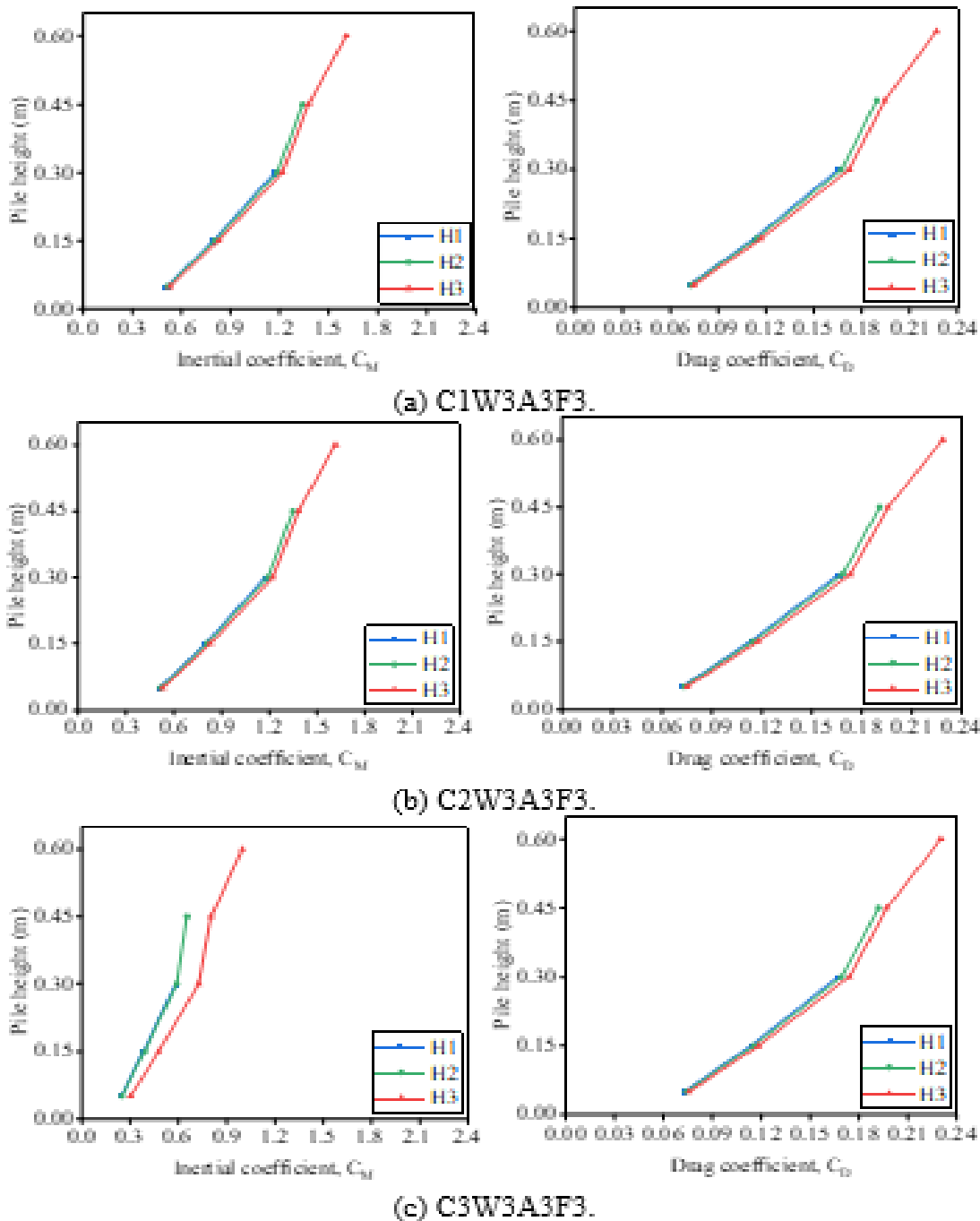


Figure 6 Inertial and drag coefficients under different water current conditions.

5.2. Results with different wave properties

The effect of different actions of water waves W1, W2 and W3 under the three water depths (H1, H2 and H3), are studied with different properties of currents, earthquake amplitudes and earthquake frequencies.

The inertial and drag coefficient of C3W1A3F3, C3W2A3F3 and C3W3A3F3, were presented in Figs. 7 (a, b and c). The three Figures show that the effect of the water waves increases the inertial and drag coefficients in a distinctive and equal manner for all the waves

studied in this research. Also, the increase of the wave is almost greater by 39%, 74% and 100% with the increase in the values of wave period W1, wave depth W2 and wave depth W3, respectively.

The behavior of hydrodynamic pressure under the influence of water waves is similar to the behavior of the effect of water currents concerning the pressure distribution along the pile. The inertial and drag coefficient behaves somewhat similarly to the hydrodynamic pressure. Take the inertial coefficient as an example, it can be seen that the coefficient changed relatively much with the increase of wave properties. For all the curves in Figs. 7 (a, b and c), the change of hydrodynamic pressure was less than 21% as the waves increased from W1 to W3.

The effect of water waves for other conditions of currents, amplitudes, and frequencies, were appeared with similar behavior to the results listed here. The results indicated that the increase of the waves is almost greater than by 15%, 11% and 1.8% with the increase in the values of the frequency, amplitude and wave, respectively.

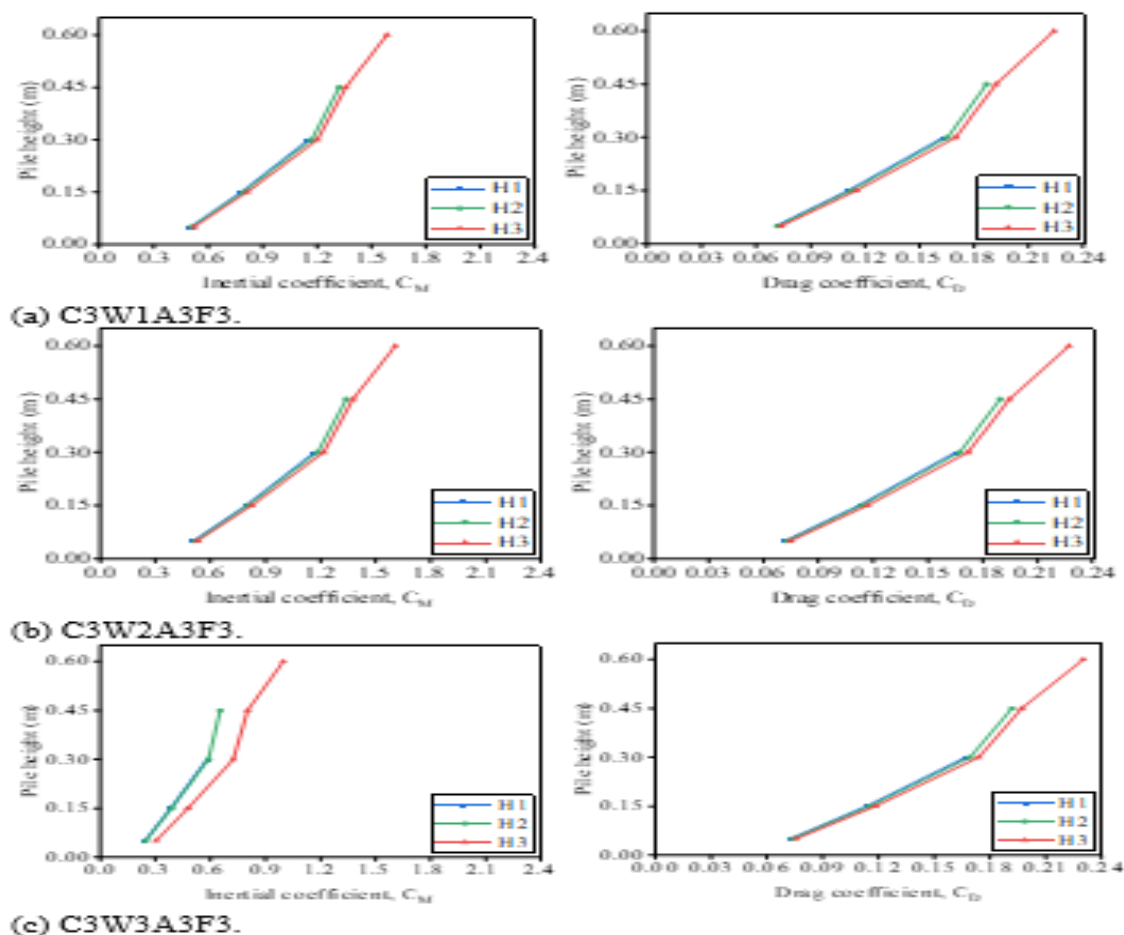


Figure 7 Inertial and drag coefficients under different water wave conditions.

5.3. Results with different earthquake amplitudes

The effect of different actions of earthquake amplitudes A1, A2 and A3 under the three water depths (H1, H2 and H3), are studied with different properties of current, wave and

earthquake frequencies.

Constant values of current, wave and frequencies were used to focus analysis of the earthquake amplitudes effect on the hydrodynamic response of the bridge foundation. The inertial and drag coefficient of C3W3A1F3, C3W3A2F3 and C3W3A3F3, were presented in Figs. 8 (a, b and c). The three Figures show that the effect of the earthquake amplitudes increases the inertial and drag coefficients for all the amplitudes studied in this research. Also, the increase of the wave is almost greater by 48.6%, 81.1%, and 100% with the increase in the values from A1, A2 and A3, respectively.

It can be noted that the coefficients changed relatively so much with the increase in earthquake amplitudes. For all the curves in Figs 8 (a, b and c), the change of hydrodynamic pressure was less than 47% as the current increasing from 0.05g to 0.2g.

The results indicated that the increase of amplitude is almost greater by 14%, 3.4%, and 1.8% with the increase in the values of the frequency, wave and current, respectively.

The effect of earthquake amplitudes for other conditions of currents, waves and frequencies, were appeared with similar behavior to the results listed here. The results indicated that the increase of the amplitudes is almost greater by 14%, 3.4%, and 1.8% with the increase in the values of the frequency, wave, and current.

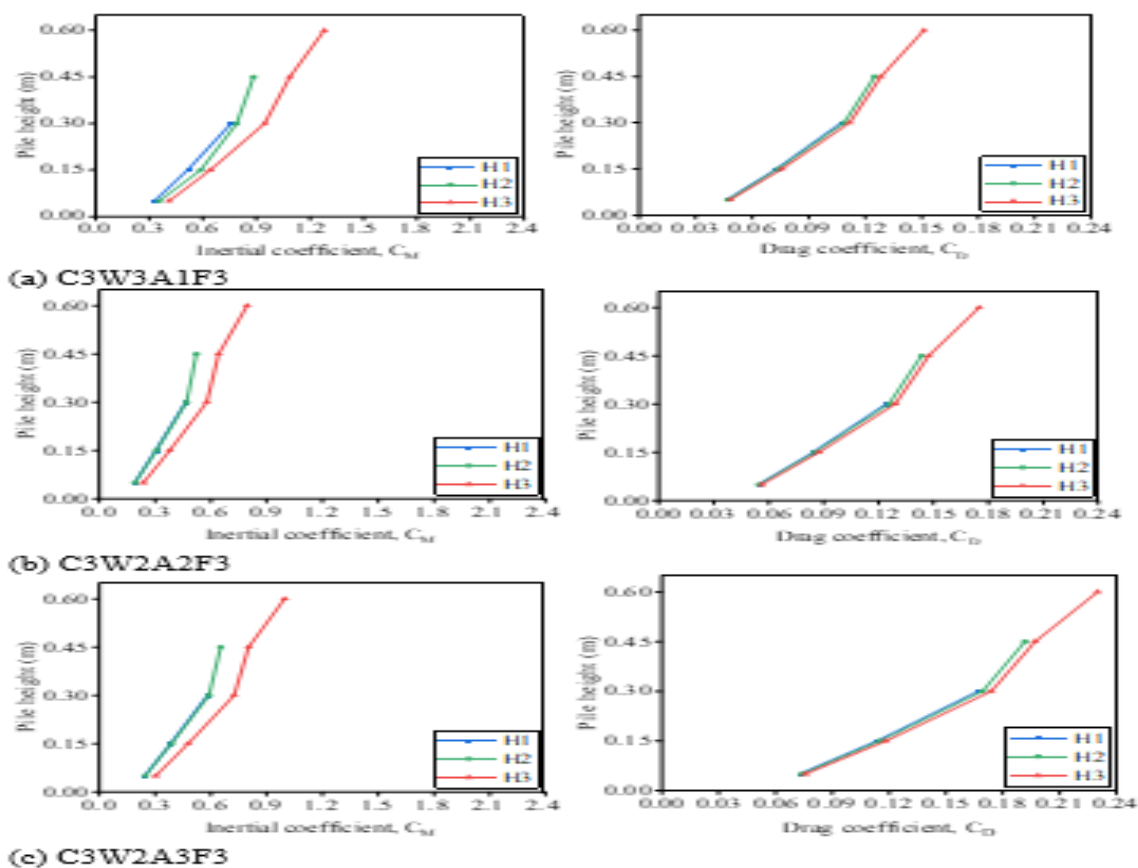


Figure 8 Inertial and drag coefficients under different earthquake amplitude actions.

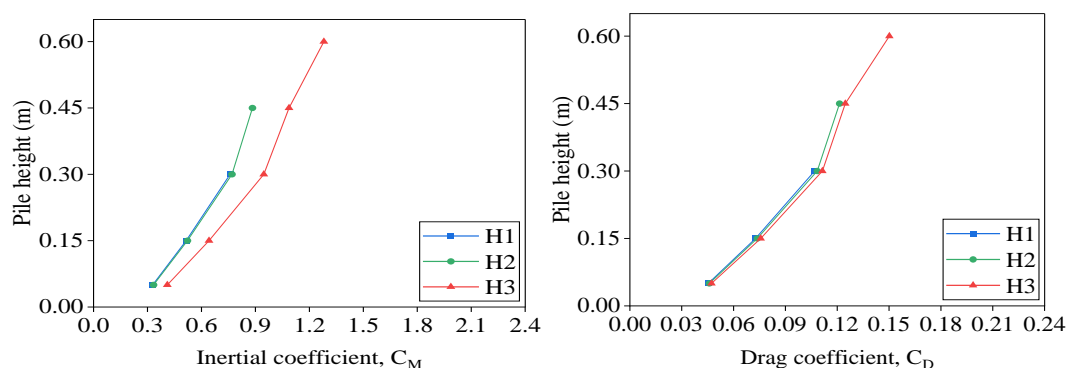
5.4. Results with different earthquake frequencies

The effect of different actions of earthquake frequencies F1, F2 and F3 under the three water depths (H1, H2 and H3), are studied with different properties of current, wave and earthquake amplitudes.

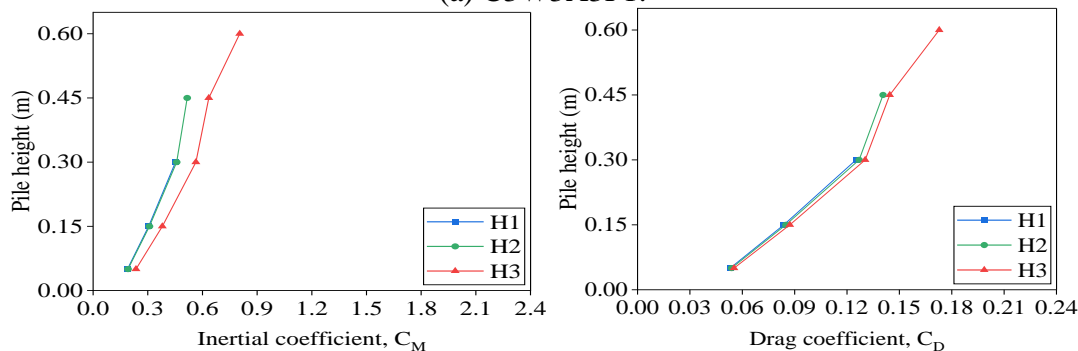
Constant values of current, wave and amplitude were used to focus analysis of the earthquake frequencies' effect on the hydrodynamic response of the bridge foundation. The inertial and drag coefficient of C3W3A3F1, C3W3A3F2 and C3W3A3F3, were presented in Figs. 9 (a, b and c). The three Figures show that the effect of the earthquake frequencies increases the inertial and drag coefficients in a distinctive and equal manner for all the frequencies studied in this research. Also, the increase of the frequencies was almost greater by 48.7%, 81.3% and 100% with the increase in the values from F1, F2 and F3, respectively.

The behavior of hydrodynamic pressure under the influence of earthquake frequencies is similar to the behavior of the effect of earthquake amplitudes on the pressure distribution along the pile. The inertial and drag coefficient behaves somewhat similarly to the hydrodynamic pressure. Take the inertial coefficient as an example, it can be seen that the coefficient changed relatively much with the increase of frequency actions. For all the curves in Figs. 9 (a, b and c), the change of hydrodynamic pressure was less than 49% as the current increasing from F1 to F3.

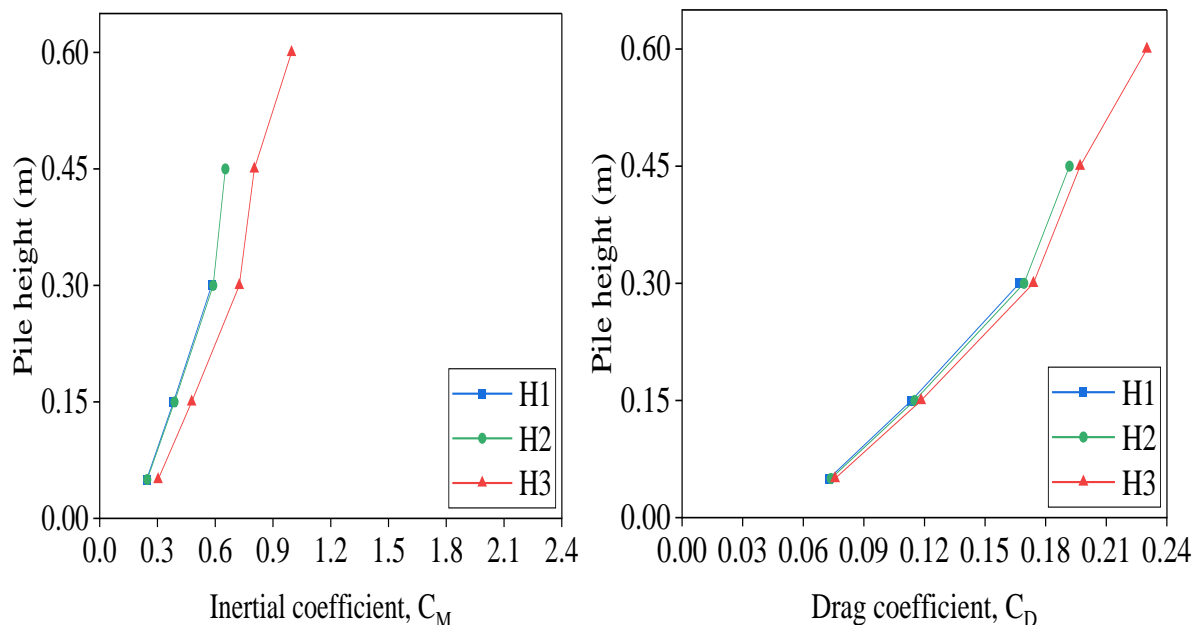
The effect of earthquake frequencies for other conditions of currents, waves and amplitudes, were appeared with similar behavior to the results listed here. The results indicated that the increase of the frequencies is almost greater by 10%, 3% and 1.5% with the increase in the values of the amplitude, wave and current, respectively, as the wave increases from F1 to F3.



(a) C3W3A3F1.



(b) C3W3A3F2.



(a) C3W3A3F3.

Figure 9 Inertial and drag coefficients under different earthquake frequency actions.

5.5. Results with different water depths

Figs 6, 7, 8 and 9 show the changing of the hydrodynamic inertial and drag coefficient with water depth under different action currents, waves, amplitudes and frequencies. It can be seen from these plots that the hydrodynamic pressure significantly increased with water depth. Therefore, the hydrodynamic mass was proportional to water depth according to Morison equation coefficients Eqs. (3) and (4).

To investigate the relationship between hydrodynamic mass and water depth, Table 3 shows the water depth and hydrodynamic mass with the test conditions at a water depth of 0.30 m, 0.45 m and 0.6 m. The mass changed with percentages of 50%, 75% and 100% as the water depth increased from H1 to H3. Also, it can be noted that the hydrodynamic mass along pile height was increased distinctively when the water depth increased from 0.3m to 0.6 m. This is due to the large mass of water transferred to the pile foundation under the influence of the mentioned conditions.

Concerning the mass changing, the frequencies, amplitudes, waves and currents are contributed first, second, third and fourth respectively.

Table 3 also showed that the hydrodynamic mass increased by 1, 2, 8.5 and 8.8 times with the action of current, waves, amplitudes, and frequencies, respectively. From this, it can be concluded that the effect of water waves is twice that of the water currents, which in turn is much less than the effect of earthquake frequencies, which are slightly greater than the effect of the earthquake amplitudes.

The interaction of waves and currents and the effect on the response of the structure must be considered for the design of an offshore structure. The existence of currents will change the wave parameters and the wave kinematics to compare with waves propagating in still water.

Table 3. *Hydrodynamic mass (kg.) with various water depths under different actions of current, waves, amplitudes and frequencies.*

Action	C1			C2			C3		
Water depth	0.3	0.45	0.6	0.3	0.45	0.6	0.3	0.45	0.6
Pile depth	Hydrodynamic mass								
0.05	0.006	0.009	0.012	0.011	0.018	0.024	0.019	0.028	0.037
0.15	0.019	0.029	0.038	0.028	0.043	0.058	0.039	0.058	0.077
0.3	0.032	0.048	0.064	0.043	0.068	0.091	0.058	0.087	0.117
0.45	-	0.067	0.089	-	0.093	0.123	-	0.117	0.157
0.6	-	-	0.115	-	-	0.156	-	-	0.197
Action	W1			W2			W3		
Water depth	0.3	0.45	0.6	0.3	0.45	0.6	0.3	0.45	0.6
Pile depth	Hydrodynamic mass								
0.05	0.012	0.019	0.025	0.025	0.038	0.051	0.037	0.057	0.075
0.15	0.038	0.057	0.076	0.056	0.087	0.116	0.076	0.118	0.155
0.3	0.063	0.096	0.127	0.088	0.136	0.181	0.115	0.179	0.234
0.45	-	0.134	0.178	-	0.185	0.247	-	0.240	0.314
0.6	-	-	0.229	-	-	0.312	-	-	0.393
Action	A1			A2			A3		
Water depth	0.3	0.45	0.6	0.3	0.45	0.6	0.3	0.45	0.6
Pile depth	Hydrodynamic mass								
0.05	0.101	0.156	0.211	0.216	0.317	0.421	0.481	0.720	0.947
0.15	0.157	0.243	0.328	0.330	0.485	0.643	0.750	1.122	1.477
0.3	0.230	0.356	0.480	0.486	0.715	0.948	1.096	1.640	2.158
0.45	-	0.380	0.513	-	0.773	1.026	-	1.800	2.368
0.6	-	-	0.647	-	-	1.288	-	-	2.779
Action	F1			F2			F3		
Water depth	0.3	0.45	0.6	0.3	0.45	0.6	0.3	0.45	0.6
Pile depth	Hydrodynamic mass								
0.05	0.117	0.162	0.217	0.222	0.324	0.434	0.500	0.739	0.985
0.15	0.166	0.251	0.336	0.339	0.489	0.648	0.745	1.099	1.486
0.3	0.246	0.373	0.499	0.517	0.757	1.012	1.111	1.640	2.187
0.45	-	0.395	0.528	-	0.795	1.063	-	1.712	2.482
0.6	-	-	0.686	-	-	1.298	-	-	2.845

5.6. Inertial and drag coefficients

The inertial and drag coefficients as discussed in the above subsections, the test results agreed well with the Morison equation coefficients as shown in Eqs. (3) and (4) for the rule of pressure mass changing with water depth, current, wave, amplitude and frequency. Based on Eq. (3), the inertial coefficient, C_M , is considered as the function of amplitude action, frequency action, and water depth, while the drag coefficient, C_D , is considered as the function of current speed, wave properties and water depth. Two dimensionless parameters are introduced in the table. One is the ratio of the diameter and height of the specimen, D/L , and the other is the ratio of the water depth and height of the specimen, H/L , which can be applied to real cylinders in coastal and offshore engineering structures. It can be concluded from Table 4 that the inertial coefficient ranged from 0.117 to 1.950 and the drag coefficient from 0.017 to 0.230 under different conditions, which varied greatly from the constant of 1.0 adopted by previous research.

The two parameters are proposed for the fitting formula of inertial and drag coefficients described below in Eqs (5) and (6):

$$C_M = 0.1785 - 0.3359 D/L + 0.0093 H/L + 0.0975 C + 0.0163 W + 2.357 A + 0.0601 F \quad (5)$$

$$C_D = 0.0263 - 0.0464 H/L + 0.0009 H/L + 0.0055 C + 0.0017 W + 0.3380 A + 0.0086 F \quad (6)$$

It was found that the inertia coefficient equation (Eq. 5) has a correlation coefficient of $R = 0.90$ and the drag coefficient equation (Eq. 6) with a correlation coefficient of $R = 0.92$, as calculated by the statistical analysis.

Table 4. *Inertial and drag coefficient values.*

No.	Case	D	L	H	D/L	H/L	C	W	A	F	CM	CD
1	C1W1A1F1	0.09	0.05	0.3	1.8	6	0.1	1	0.05	2	0.117	0.017
2			0.15		0.6	2					0.196	0.028
3			0.3		0.3	1					0.294	0.042
4			0.05	0.45	1.8	9					0.118	0.017
5			0.15		0.6	3					0.198	0.028
6			0.3		0.3	1.5					0.298	0.042
7			0.45		0.2	1					0.334	0.047
8	C1W1A1F1	0.09	0.05	0.6	1.8	12	0.1	1	0.05	2	0.122	0.017
9			0.15		0.6	4					0.204	0.029
10			0.3		0.3	2					0.306	0.043
11			0.45		0.2	1.333					0.343	0.048
12			0.6		0.15	1					0.439	0.062
.
.
.
961	C3W3A3F3	0.09	0.05	0.3	1.8	6	0.4	3	0.2	8	0.514	0.073
962			0.15		0.6	2					0.804	0.114
963			0.3		0.3	1					1.181	0.167
964			0.05	0.45	1.8	9					0.521	0.074
965			0.15		0.6	3					0.815	0.115
966			0.3		0.3	1.5					1.198	0.169
967			0.45		0.2	1					1.357	0.192
968	C3W3A3F3	0.09	0.05	0.6	1.8	12	0.4	3	0.2	8	0.641	0.076
969			0.15		0.6	4					1.002	0.118
970			0.3		0.3	2					1.473	0.174
971			0.45		0.2	1.333					1.669	0.197
972			0.6		0.15	1					1.950	0.230

4. Conclusion

Morison equation was modified to study the changing rule of the hydrodynamic pressure along the height of pile foundation subjected to combined current, wave and earthquake actions. Inertial and drag coefficients were calculated by simplifying inertia force and drag force, respectively. To comprehensively analyze these coefficients, a series of hydrodynamic experimental tests were conducted as a function of different conditions of water depths, current velocities, wave properties, earthquake amplitudes and earthquake frequencies.

The conclusion can be summarized as follows:

- (1) The hydrodynamic pressure significantly increases as water depth increases. The hydrodynamic mass along pile height was changed with a percentage of 50% to 100% as the water depth changed from 0.3m to 0.6m.
- (2) The effect of the water current increases the inertial and drag coefficients in a distinctive and equal manner for all the currents studied in this research. The increased of the current speed is almost greater by 31%, 68%, 100% with the changed values 0.1m/sec, 0.2m/sec and 0.4m/sec, respectively.
- (3) Water waves increase the inertial and drag coefficients with percent 39%, 74%, and 100% with the increase in the values of wave period, wave depth, wavelength, respectively.
- (4) The three studied earthquake amplitudes (0.05, 0.1 and 0.2) g showed increases in the inertial and drag values by 48.6%, 81.1%, and 100%, respectively.
- (5) The effect of earthquake frequencies has appeared distinctively for all the frequencies studied in this research. The increases in the frequencies are almost greater by 48.7%, 81.3%, and 100% with the increase in the values 2 Hz, 4 Hz and 8 Hz, respectively.
- (6) Hydrodynamic pressure of the pile increases from bottom to top and for all the studied conditions, this is due to the effect of the compressed mass of water that results from impacted water loads from the bottom to the water surface.
- (7) In general, it can be concluded that the inertial coefficient has the same changing rule as the drag coefficient. The inertial coefficient ranged from 0.117 to 1.950 and the drag coefficient ranged from 0.017 to 0.230 under various studied conditions, which differs significantly from the constant of 1.0 assumed by previous research.

The results of this study can provide a reference for the application of the Morison equation in calculating the inertial and drag coefficients under current wave water loads during earthquake actions.

5. Acknowledgements

The authors gratefully acknowledge support for this research from the Ministry of Higher Education and Scientific Research-University of Technology Laboratories, Iraq.

6. Funding

The research paper has not been funded by any public, academic, industrial, or financial entity.6819

Compliance with Ethical Standards Conflict of interest

The authors declare no conflict of interest.

Data Availability

The data of this study are available from the corresponding author upon request.

References

- Al-Taie, A.J. and Albusoda, B.S., (2019). Earthquake hazard on Iraqi soil: Halabjah earthquake as a case study. *Geodesy and Geodynamics*, 10(3), pp.196-204.
- An-jie, W. and Wan-li, Y., (2020). Numerical study of pile group effect on the hydrodynamic
- Res Militaris*, vol.12, n°2, Summer-Autumn 2022

- force on a pile of sea-crossing bridges during earthquakes. *Ocean Engineering*, 199, p.106999.
- Ding, Y., Ma, R., Shi, Y.D. and Li, Z.X., (2018). Underwater shaking table tests on bridge pier under combined earthquake and wave-current action. *Marine Structures*, 58, pp.301-320.
- Fang, Q., Hong, R., Guo, A., Stansby, P.K. and Li, H., (2018). Analysis of hydrodynamic forces acting on submerged decks of coastal bridges under oblique wave action based on potential flow theory. *Ocean Engineering*, 169, pp.242-252.
- Gao, L.I.N., Tong, Z.H.U. and Bei, L.I.N., (2000). Similarity technique for dynamic structural model test. *JOURNAL-DALIAN UNIVERSITY OF TECHNOLOGY*, 40(1), pp.1-8.
- Goto, H., Toki, K., (1965). Vibration characteristics and aseismic design of submerged bridge piers. In: *Proceedings of the 3rd World Conference on Earthquake Engineering*
- Harris, H.G. and Sabnis, G., (1999). *Structural modeling and experimental techniques*. CRC press.
- Konstantinidis, E. and Bouris, D., (2017). Drag and inertia coefficients for a circular cylinder in steady plus low-amplitude oscillatory flows. *Applied Ocean Research*, 65, pp.219-228.
- Li, F.R., Chen, G.X. and Wang, Z.H., (2010), January. The Earthquake Hydrodynamic Pressure Effects Analysis of the Large Bridge Group Piles Foundation Based on ABAQUS Software. In *2010 Second International Conference on Computer Modeling and Simulation* (Vol. 4, pp. 220-225). IEEE.
- Li, Q. and Yang, W., (2013). An improved method of hydrodynamic pressure calculation for circular hollow piers in deep water under earthquake. *Ocean Engineering*, 72, pp.241-256.
- Li, Z.X., Wu, K., Shi, Y., Li, N. and Ding, Y., (2018). Coordinative similitude law considering fluid-structure interaction for underwater shaking table tests. *Earthquake Engineering & Structural Dynamics*, 47(11), pp.2315-2332.
- Li, Z.X., Wu, K., Shi, Y., Ning, L. and Yang, D., (2019). Experimental study on the interaction between water and cylindrical structure under earthquake action. *Ocean Engineering*, 188, p.106330.
- Liu, S.X., Li, Y.C. and Li, G.W., (2007). Wave current forces on the pile group of base foundation for the East Sea Bridge, China. *Journal of Hydrodynamics, Ser. B*, 19(6), pp.661-670.
- Martinelli, L., Barbella, G. and Feriani, A., (2011). A numerical procedure for simulating the multi-support seismic response of submerged floating tunnels anchored by cables. *Engineering structures*, 33(10), pp.2850-2860.
- Morison, J.R., Johnson, J.W. and Schaaf, S.A., (1950). The force exerted by surface waves on piles. *Journal of Petroleum Technology*, 2(05), pp.149-154.
- Penzien, J. and Kaul, M.K., (1972). Response of offshore towers to strong motion earthquakes. *Earthquake Engineering & Structural Dynamics*, 1(1), pp.55-68.
- Raed, K. and Soares, C.G., (2018). Variability effect of the drag and inertia coefficients on the Morison wave force acting on a fixed vertical cylinder in irregular waves. *Ocean Engineering*, 159, pp.66-75.
- Song, B., Zheng, F. and Li, Y., (2013). Study on a simplified calculation method for hydrodynamic pressure to slender structures under earthquakes. *Journal of earthquake engineering*, 17(5), pp.720-735.
- Teng, C.C. and Nath, J.H., (1985). Forces on horizontal cylinder towed in waves. *Journal of waterway, port, coastal, and ocean engineering*, 111(6), pp.1022-1040.
- Vengatesan, V., Varyani, K.S. and Barltrop, N., (2000). An experimental investigation of hydrodynamic coefficients for a vertical truncated rectangular cylinder due to regular

- and random waves. *Ocean Engineering*, 27(3), pp.291-313.
- Wang, P., Zhao, M., Du, X. and Liu, J., (2019). Dynamic response of bridge pier under combined earthquake and wave–current action. *Journal of Bridge Engineering*, 24(10), p.04019095.
- Wei, K., Yuan, W. and Bouaanani, N., (2013). Experimental and numerical assessment of the three-dimensional modal dynamic response of bridge pile foundations submerged in water. *Journal of Bridge Engineering*, 18(10), pp.1032-1041.
- Yang, W. and Li, Q., (2013). The expanded Morison equation considering inner and outer water hydrodynamic pressure of hollow piers. *Ocean Engineering*, 69, pp.79-87.
- Yuan, Z.D. and Huang, Z.H., (2010). An experimental study of inertia and drag coefficients for a truncated circular cylinder in regular waves. *Journal of Hydrodynamics*, 22(1), pp.313-318.
- Zheng, X.Y., Li, H., Rong, W. and Li, W., (2015). Joint earthquake and wave action on the monopile wind turbine foundation: An experimental study. *Marine Structures*, 44, pp.125-141.